

Kinetic study on the direct nitridation of silicon powders diluted with α - Si_3N_4 at normal pressure

Shao-wu Yin^{1,2)}, Li Wang^{1,2)}, Li-ge Tong^{1,2)}, Fu-ming Yang¹⁾, and Yan-hui Li¹⁾

1) School of Mechanical Engineering, University of Science and Technology Beijing, Beijing 100083, China

2) Beijing Key Laboratory of Energy Saving and Emission Reduction for Metallurgical Industry, University of Science and Technology Beijing, Beijing 100083, China

(Received: 18 July 2012; revised: 10 August 2012; accepted: 12 October 2012)

Abstract: Silicon nitride (Si_3N_4) powders were prepared by the direct nitridation of silicon powders diluted with α - Si_3N_4 at normal pressure. Silicon powders of 2.2 μm in average diameter were used as the raw materials. The nitriding temperature was from 1623 to 1823 K, and the reaction time ranged from 0 to 20 min. The phase compositions and morphologies of the products were analyzed by X-ray diffraction and scanning electron microscopy, respectively. The effects of nitriding temperature and reaction time on the conversion rate of silicon were determined. Based on the shrinking core model as well as the relationship between the conversion rate of silicon and the reaction time at different temperatures, a simple model was derived to describe the reaction between silicon and nitrogen. The model revealed an asymptotic exponential trend of the silicon conversion rate with time. Three kinetic parameters of silicon nitridation at atmospheric pressure were calculated, including the pre-exponential factor ($2.27 \text{ cm}\cdot\text{s}^{-1}$) in the Arrhenius equation, activation energy ($114 \text{ kJ}\cdot\text{mol}^{-1}$), and effective diffusion coefficient ($6.2\times 10^{-8} \text{ cm}^2\cdot\text{s}^{-1}$). A formula was also derived to calculate the reaction rate constant.

Keywords: silicon nitride; powders; nitridation; reaction kinetics; activation energy

1. Introduction

Silicon nitride (Si_3N_4) has excellent properties, such as high strength retention at high temperature, good thermal shock resistance, high temperature deformation resistance, and high corrosion resistance. Thus, Si_3N_4 is one of the most promising structural materials for high temperature and high mechanical stress applications. Some typical applications of Si_3N_4 ceramics include gas turbine components, pistons and cylinder liners, turbocharger rotors, high temperature bearings, high speed cutting tools, etc. [1-3]. One of the most common methods for preparing Si_3N_4 ceramics is hot press sintering, which uses Si_3N_4 powders mixed with a small amount of sintering additives as raw materials.

Currently, the main approaches to the preparation of Si_3N_4 powders include carbothermal reduction [4], gas phase reaction [5], thermal decomposition [6], and direct nitridation of silicon (Si) powders [7-8]. However, carbo-

thermal reduction produces a large amount of silicon carbide, the gas phase reaction requires high cost materials, and the thermal decomposition process is too complex to control. In contrast to these methods, the direct nitridation of Si powders is simple, cost-effective, and suitable for industrial production. Thus, this process is becoming one of the main methods for preparing Si_3N_4 powders.

During the direct nitridation of Si powders, the intrinsic reaction rate can be remarkably improved by increasing the nitriding temperature. However, when the temperature exceeds the melting point of Si (i.e., 1683 K), Si powders melt and condense together, which reduces the reactive surface and hinders further reaction [9-10]. The condensation of liquid Si can be prevented by adding Si_3N_4 diluent in the process of self-propagating high-temperature synthesis [11].

In this work, Si_3N_4 powders were prepared by the direct nitridation of Si powders diluted with α - Si_3N_4 at

Corresponding author: Shao-wu Yin E-mail: yinsw@ustb.edu.cn

atmospheric pressure. The phase compositions and morphologies of the products were analyzed by X-ray diffraction (XRD) and scanning electron microscopy (SEM), respectively. The effects of nitriding temperature and reaction time on the Si conversion rate were investigated. Based on the shrinking core model as well as the relationship between the Si conversion rate and reaction time at different temperatures, a simple model was derived to describe the reaction between Si and nitrogen (N_2).

2. Experimental

2.1. Experimental materials

Si powders (2.2 μm in average diameter and 99.9% purity) were used as the raw materials, and $\alpha\text{-Si}_3\text{N}_4$ powders (2.2 μm in average diameter and 99.0% purity) were used as the diluent. Nitrogen (99.99% purity) was used as the reaction gas.

2.2. Experimental apparatus

Fig. 1 shows the schematic diagram of the experimental apparatus, which mainly consists of a resistance furnace, a reaction chamber, and a gas supply system. The resistance furnace was heated by Si molybdenum rods, which can provide the highest temperature of 1873 K as measured by an S-type thermocouple. The reaction chamber is a ceramic tube with an inner diameter of 30 mm and a length of 1000 mm. The gas supply system is composed of a N_2 cylinder, a reducing valve, a flowmeter, some rubber pipes, and a corundum pipe.

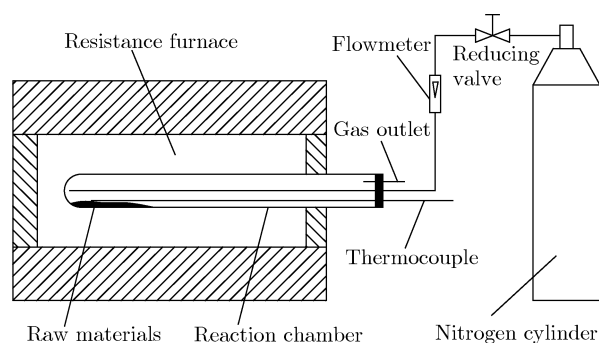


Fig. 1. Schematic diagram of the experimental apparatus.

2.3. Experimental schedule

The dried Si and $\alpha\text{-Si}_3\text{N}_4$ powders were uniformly mixed according to a predetermined mass proportion (50wt% Si and 50wt% $\alpha\text{-Si}_3\text{N}_4$). The mixtures were then placed at the bottom of the reaction chamber, and N_2 was introduced into the reaction chamber at a flow rate of 2.0 $\text{L}\cdot\text{min}^{-1}$ to replace air in the chamber. The process of gas exchange lasted for 20 min. The reaction chamber was placed on the hearth of the furnace, which had been heated to different predetermined temperatures (1623, 1673, 1723,

1773, and 1823 K). The flow rate of N_2 was maintained at 400 $\text{mL}\cdot\text{min}^{-1}$. After predetermined nitriding times (5, 10, 15, and 20 min), the chamber was removed and cooled to room temperature in air.

2.4. Quantitative determination

The phase content of α - and $\beta\text{-Si}_3\text{N}_4$ in the products was determined by a normalizing method proposed by Zhou [12], which had the advantages of eliminating the preferred orientation, good reproducibility, and small error. This quantitative determination method was adopted by Li *et al.* [13]. Once the phase content is determined, the conversion rate of Si powders can be calculated according to the following equation:

$$X_{\text{Si}} = \frac{1 - \frac{m_{\text{Si}}}{1 - m_{\alpha}}}{1 + \frac{2}{3}m_{\text{Si}}} \quad (1)$$

where X_{Si} is the conversion rate of Si powders, m_{Si} the mass fraction of Si in the products, and m_{α} the mass fraction of $\alpha\text{-Si}_3\text{N}_4$ diluent in the raw materials.

3. Results and discussion

3.1. XRD analysis

When the added proportion of $\alpha\text{-Si}_3\text{N}_4$ is 50wt% and the nitriding time is 10 min, the XRD patterns of the experimental products at different nitriding temperatures are shown in Fig. 2. The products mainly include Si, $\alpha\text{-Si}_3\text{N}_4$, and $\beta\text{-Si}_3\text{N}_4$, in which $\alpha\text{-Si}_3\text{N}_4$ is the dominant and popular phase because of its better sintering properties. Combined with the above quantitative determination method, when the nitriding temperature increases from 1623 to 1823 K, the conversion rate of Si powders increases from 65.4% to 92.5%, the amount of $\beta\text{-Si}_3\text{N}_4$ in the products also increases from 10.4wt% to 28.2wt%, and the amount of unreacted Si in the products decreases from 14.2wt% to 2.8wt%. These phenomena indicate that an increased

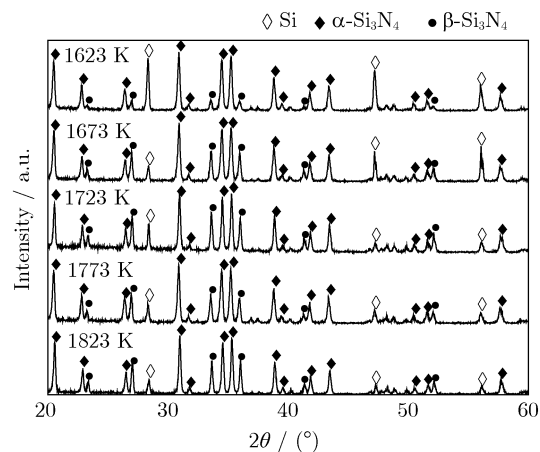


Fig. 2. XRD patterns of the products at different nitriding temperatures (10 min, 50wt% $\alpha\text{-Si}_3\text{N}_4$ diluent).

nitriding temperature results in not only an increased conversion rate of Si powders but also an increased β -Si₃N₄ content. To decrease the β -Si₃N₄ content, the nitriding temperature should be properly controlled.

3.2. SEM analysis

When the added proportion of α -Si₃N₄ is 50wt% and the nitriding time is 10 min, the SEM image of the products at the nitriding temperature of 1823 K is shown in Fig. 3. Most of the products exhibit spherical morphologies, although some are columnar, whisker-shaped or cluster-shaped particles. Without the addition of α -Si₃N₄ diluent, liquid Si agglomerates and forms a large Si block when Si powders melt. Consequently, the reactive surface area decreases. Given that the added proportion of α -Si₃N₄ is high, Si powders are effectively separated. Agglomeration between the particles does not occur and the particles are uniformly dispersed.

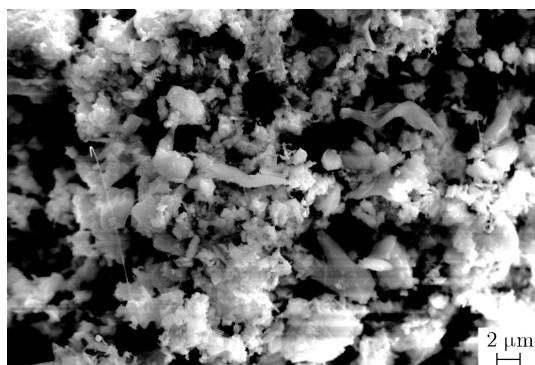


Fig. 3. SEM image of the products (1823 K, 10 min, 50wt% α -Si₃N₄ diluent).

3.3. Analysis of Si conversion rate

Fig. 4 shows relationships between the Si conversion rate and reaction holding time at different temperatures with 50wt% α -Si₃N₄ added. The conversion rate of Si powders gradually increases with the increase in nitriding time.

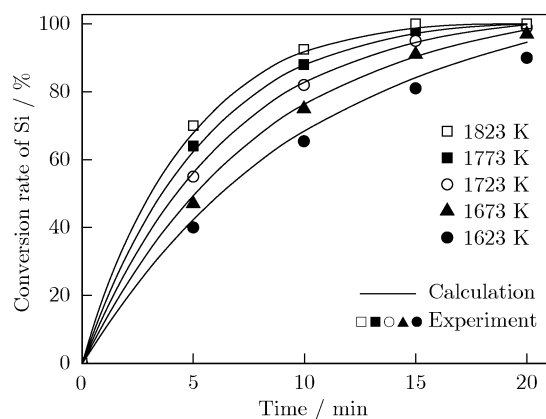


Fig. 4. Relationships between the Si conversion rate and reaction time.

When the temperature increases from 1623 to 1823 K at the nitriding time of 10 min, the conversion of Si powders remarkably increases from 65.4% to 92.5%. Therefore, increasing the nitriding temperature can significantly increase the nitridation rate, which is conducive to the initial stage of nitriding reaction. However, the influence of temperature on the nitridation rate is not very significant at the final stage of the reaction.

4. Theoretical model and calculation

4.1. Model of the reaction between Si and N₂

Different reaction conditions and the relatively unclear nitridation reaction mechanism have prompted researchers to use different kinetic methods for the Si-N₂ reaction. Different models have also been proposed to describe the transformation from Si powders to Si₃N₄ powders. Jovanovic [14] suggested that the conversion rate of Si could be fitted with the asymptotic exponential law. Yagi and Kunii [15] used the shrinking core model to study the combustion of carbon particles. Pigeon and Varma [16] investigated the nitridation of Si powders using the sharp interface model.

The following reaction between Si and N₂ proceeds at high temperature:



When the nitriding temperature is higher than the melting point of Si (1683 K), Si particles melt and evaporate at the beginning of the nitridation reaction. The gas-liquid reaction and chemical vapor deposition reaction occur to produce Si₃N₄, which coats the surface of Si particles. Once the coated product layers are formed on the surface of Si particles, N₂ diffuses onto the surface of the unreacted Si core through the product layers. The gas-liquid reaction between N₂ (g) and Si (l) occurs to generate Si₃N₄. When the nitriding temperature is less than the melting point of Si, a gas-solid reaction between N₂ (g) and Si (s) occurs to produce Si₃N₄. For simplicity, the traditional gas-solid reaction mechanism is used to build the Si-N₂ reaction model. The simulation results agree with the experimental data.

In this article, the shrinking core model with constant particle size is used to create the Si-N₂ reaction model. This model involves three steps: gas film diffusion, solid product layer diffusion, and surface chemical reaction. Thus, three kinds of resistances are observed: gas film diffusion resistance, solid product layer diffusion resistance, and chemical kinetic resistance. The reaction rate equation for a single spherical particle is shown in Eq. (3) [17]:

$$r_A = \frac{f}{f_g + f_s + f_r} \quad (3)$$

where r_A is the reaction rate, mol·s⁻¹; f the total driving force, mol·cm⁻³; f_g the gas film diffusion resistance,

$\text{s}\cdot\text{cm}^{-3}$; f_s the solid product layer diffusion resistance, $\text{s}\cdot\text{cm}^{-3}$; and f_r the chemical kinetic resistance, $\text{s}\cdot\text{cm}^{-3}$.

The expressions of the driving force and resistance are shown in Eq. (4) [17]:

$$\left\{ \begin{array}{l} f = c_{\text{ag}} \\ f_g = \frac{1}{4\pi R_p^2 k_g} \\ f_s = \frac{(1 - X_{\text{Si}})^{-1/3} - 1}{4\pi R_p D_e} \\ f_r = \frac{1}{4\pi R_p^2 (1 - X_{\text{Si}})^{2/3} k_s} \end{array} \right. \quad (4)$$

where c_{ag} is the concentration of N_2 calculated by the ideal gas equation, $\text{mol}\cdot\text{cm}^{-3}$; R_p the average radius of Si particles, cm ; k_g the gas phase mass transfer coefficient, $\text{cm}\cdot\text{s}^{-1}$; D_e the effective diffusion coefficient of N_2 within the solid product layer, $\text{cm}^2\cdot\text{s}^{-1}$; and k_s the reaction rate constant based on the unit reaction interface, $\text{cm}\cdot\text{s}^{-1}$.

In the present study, increasing the flow rate of N_2 does not change the reaction rate, so the gas film diffusion

resistance f_g can be ignored. Therefore, only the product layer diffusion resistance f_s and chemical kinetic resistance f_r are considered in the reaction rate.

4.2. Calculation of kinetic parameters

(1) Nitriding temperature lower than the melting point of Si

At the nitriding temperature of 1623 K (lower than the melting point of Si), the chemical reaction rate is slow, the Si_3N_4 product layer is thin, and the diffusion resistance in the product layer can be ignored. Thus, the reaction is a type of chemical kinetic control on the interface. The relationship between the reaction time and Si conversion rate can be determined by Eq. (5) [17]:

$$\tau = \frac{\rho_{\text{Si}} R_p}{b M_{\text{Si}} k_s c_{\text{ag}}} \left[1 - (1 - X_{\text{Si}})^{\frac{1}{3}} \right] \quad (5)$$

where τ is the reaction time, s ; ρ_{Si} the density of Si, $\text{g}\cdot\text{cm}^{-3}$; b the ratio of the stoichiometric coefficients in Eq. (2), and M_{Si} the molecular weight of Si, $\text{g}\cdot\text{mol}^{-1}$. The values of these variables are listed in Table 1.

Table 1. Values of variables in Eq. (5)

$\rho_{\text{Si}} / (\text{g}\cdot\text{cm}^{-3})$	R_p / cm	b	$M_{\text{Si}} / (\text{g}\cdot\text{mol}^{-1})$	$p_{\text{N}_2} / \text{Pa}$	$R_g / (\text{J}\cdot\text{mol}^{-1}\cdot\text{K}^{-1})$	$c_{\text{ag}} / (\text{mol}\cdot\text{cm}^{-3})$
2.329	1.1×10^{-4}	1.5	28	1.01×10^5	8.314	7.5×10^{-6} (at 1623 K)

Note: $c_{\text{ag}} = p_{\text{N}_2} / (R_g T)$.

Values in Table 1 can be used to derive Eq. (6) from Eq. (5):

$$\tau = \frac{0.81}{k_s} \left[1 - (1 - X_{\text{Si}})^{\frac{1}{3}} \right] \quad (6)$$

Eq. (6) is used to fit the experimental data at 1623 K (Fig. 4), and the reaction rate constant can be calculated, i.e., $k_{s1} = 4.87 \times 10^{-4} \text{ cm}\cdot\text{s}^{-1}$ at 1623 K. Then k_{s1} is input into Eq. (6) to calculate the Si conversion rate at 1623 K. The calculated and experimental results are consistent, and the curve is shown in Fig. 4.

(2) Nitriding temperature higher than the melting point of Si

At different nitriding temperatures of 1673, 1723, 1773, and 1823 K, given the relatively higher temperature than the melting point of Si, the reaction rate increases. The chemical kinetic resistance f_r and diffusion resistance f_s in the product layer cannot be ignored. Thus, the relationship between the reaction time and the Si conversion rate can be determined by Eq. (7) [17]:

$$\frac{b M_{\text{Si}} c_{\text{ag}}}{\rho_{\text{Si}} R_p} \tau = \frac{1}{k_s} \left[1 - (1 - X_{\text{Si}})^{\frac{1}{3}} \right] + \frac{R_p}{6 D_e} \left[1 - 3(1 - X_{\text{Si}})^{\frac{2}{3}} + 2(1 - X_{\text{Si}}) \right] \quad (7)$$

Eq. (7) is used to fit the experimental data at 1773

K (Fig. 4), and the effective diffusion coefficient of N_2 and the reaction rate constant can be calculated, i.e., $D_e = 6.2 \times 10^{-8} \text{ cm}^2\cdot\text{s}^{-1}$ and $k_{s2} = 9.95 \times 10^{-4} \text{ cm}\cdot\text{s}^{-1}$ at 1773 K. Then k_{s2} , D_e , and other data are input into Eq. (7) to calculate the Si conversion rate at 1773 K. The calculated curve at 1773 K exhibits an asymptotic exponential trend (Fig. 4), which is consistent with the finding of Jovanovic [14].

The activation energy E ($114 \text{ kJ}\cdot\text{mol}^{-1}$) and pre-exponential factor k_{s0} ($2.27 \text{ cm}\cdot\text{s}^{-1}$) are then calculated by inputting the values of k_{s1} at 1623 K and k_{s2} at 1773 K into the Arrhenius equation: $k_s = k_{s0} \exp(-E/RT)$.

Therefore, the reaction rate constant k_s at any temperature can be calculated according to

$$k_s = 2.27 \exp \left(-\frac{114000}{8.314T} \right) \quad (8)$$

Assuming that the effective diffusion coefficient of N_2 (D_e) does not change with temperature, k_s , D_e , and other data are inputted into Eq. (7) to calculate the Si conversion rate at 1673, 1723, and 1823 K. The calculated and experimental results are consistent, and the curves are shown in Fig. 4. An asymptotic exponential trend is observed, consistent with the finding of Jovanovic [14].

In the Arrhenius equation, the index factor $\exp(-E/RT)$ plays a critical role in the reaction rate constant k_s . The core of the index factor is the activation

energy E , so determining the activation energy is an important step in kinetic analysis. However, since different experimental conditions and research methods are used by researchers, the obtained activation energy values are not the same. Under experimental conditions in this article, the activation energy is 114 kJ·mol⁻¹, which is within the obtained range (54-777 kJ·mol⁻¹) by other researchers [14, 18-20].

Yang *et al.* [21] demonstrated that the conversion rate of Si powders could be considerably improved by increasing the added proportion of α -Si₃N₄ diluent. In particular, when the added proportion of α -Si₃N₄ increases from 10wt% to 50wt%, the conversion rate of Si powders increases from 38% to 92.5% and the amount of unreacted Si decreases from 45.4wt% to 2.8wt%. These phenomena indicate that α -Si₃N₄ can induce the separation of Si powders and reduce the condensation of liquid Si. Consequently, the reactive surface area and the Si conversion rate increase.

Therefore, the addition of α -Si₃N₄ can prevent the agglomeration of liquid Si and decrease the activation energy, which is conducive to the nitridation reaction, consistent with the finding of Yang *et al.* [21]. The role of the added proportion of α -Si₃N₄ diluent in the kinetic model and the kinetic mechanism of this diluent require further study.

5. Conclusions

(1) The contents of α - and β -Si₃N₄ products gradually increased with the nitriding temperature increasing. When the temperature increased from 1623 to 1823 K with the nitriding time of 10 min, the conversion rate of Si powders remarkably increased from 65.4% to 92.5%.

(2) Based on the shrinking core model as well as the relationship between the Si conversion rate and reaction time at different temperatures, a simple model was derived to describe the reaction between Si and N₂. The model revealed an asymptotic exponential trend of the silicon conversion rate with time.

(3) Some kinetic parameters of Si powders nitridation at atmospheric pressure were calculated. The parameters were the pre-exponential factor (2.27 cm·s⁻¹) in the Arrhenius equation, activation energy (114 kJ·mol⁻¹), and effective diffusion coefficient (6.2×10⁻⁸ cm²·s⁻¹). A formula was also derived to calculate the reaction rate constant.

(4) The addition of α -Si₃N₄ diluent can prevent the agglomeration of liquid Si but decrease the activation energy, which is conducive to the nitridation reaction.

Acknowledgements

This work was financially supported by the Natural Science Foundation of China (No. 51106008) and the Major State Basic Research and Development Program of

China (No. 2012CB720406).

References

- [1] F.L. Riley, Silicon nitride and related materials, *J. Am. Ceram. Soc.*, 83(2000), No. 2, p. 245.
- [2] L. Bai, X.D. Mao, W.P. Shen, and C.C. Ge, Comparative study of β -Si₃N₄ powders prepared by SHS sintered by spark plasma sintering and hot pressing, *J. Univ. Sci. Technol. Beijing*, 14(2007), No. 3, p. 271.
- [3] Y.H. Li, L. Wang, S.W. Yin, F.M. Yang, and P. Wu, Rapid crystallization process of amorphous silicon nitride, *J. Am. Ceram. Soc.*, 94(2011), No. 12, p. 4169.
- [4] R. Koc and S. Kaza, Synthesis of α -Si₃N₄ from carbon coated silica by carbothermal reduction and nitridation, *J. Eur. Ceram. Soc.*, 18(1998), No. 10, p. 1471.
- [5] T.A. Jennett, P.D. Harmsworth, and A.G. Jones, Ultra fine crystalline silicon nitride from a continuous gas phase plasma route, *Key Eng. Mater.*, 89-91(1994), p. 47.
- [6] G.M. Crosbie and W.J. Smothers, Preparation of silicon nitride powders, [in] *Proceedings of the 13th Automotive Materials Conference: Ceramic Engineering and Science Proceedings*, Vol. 7, Iss. 9/10, John Wiley & Sons Inc., 1986, p. 1144.
- [7] J. Chen, J. Yang, S.W. Yin, and L. Wang, Numerical simulation on thermal process in an Si₃N₄-reaction furnace with CFX, *J. Univ. Sci. Technol. Beijing*, 27(2005), No. 6, p. 710.
- [8] V.V. Zakorzhevskii and I.P. Borovinskaya, Combustion synthesis of silicon nitride using ultrafine silicon powders, *Powder Metall. Met. Ceram.*, 48(2009), No. 7-8, p. 375.
- [9] A. Varma, R.G. Pigeon, and A.E. Miller, Kinetics of α - and β -Si₃N₄ formation from oxide-free high-purity Si powder, *J. Mater. Sci.*, 26(1991), No. 16, p. 4541.
- [10] M. Maalmi and A. Varma, Intrinsic nitridation kinetics of high-purity silicon powder, *AIChE J.*, 42(1996), No. 12, p. 3477.
- [11] Y.X. Chen, Z.M. Lin, J.T. Li, J.S. Du, and S.L. Yang, PTFE, an effective additive on the combustion synthesis of silicon nitride, *J. Eur. Ceram. Soc.*, 28(2008), No. 1, p. 289.
- [12] H.P. Zhou, Introduction to the method of quantitative determination of phase content of Si₃N₄ by X-ray diffraction analysis, *J. Chin. Ceram. Soc.*, 8(1980), No. 4, p. 414.
- [13] X.L. Li, X.L. Chen, H.M. Ji, X.H. Sun, and L.G. Zhao, Phase analysis and thermal conductivity of in situ O'-sialon/ β -Si₃N₄ composites, *Int. J. Miner. Metall. Mater.*, 19(2012), No. 8, p. 757.
- [14] Z.R. Jovanovic, Kinetics of direct nitridation of pelletized silicon grains in a fluidized bed: experiment, mechanism and modelling, *J. Mater. Sci.*, 33(1998), No. 9, p. 2339.

- [15] S. Yagi and D. Kunii, Studies on combustion of carbon particles in flames and fluidized beds, [in] *Proceedings of the 5th International Symposium on Combustion*, New York, 1955, p. 231.
- [16] R.G. Pigeon and A. Varma, Quantitative kinetic analysis of silicon nitridation, *J. Mater. Sci.*, 28(1993), No. 11, p. 2999.
- [17] K.B. Luo, M.H. Luo, and L.P. Li, *Reaction Engineering Principle*, Science Press, Beijing, 2005, p. 285.
- [18] H.N. Huang, Formation mechanism and kinetics of α - and β -Si₃N₄, *Ceram. Stud. J.*, 11(1996), No. 1, p. 16.
- [19] H.M. Jennings, On reactions between silicon and nitrogen, *J. Mater. Sci.*, 18(1983), No. 4, p. 951.
- [20] S.W. Yin, L. Wang, L.G. Tong, F.M. Yang, and Y.H. Li, Kinetics analysis of direct nitridation of silicon powders at atmospheric pressure, *Adv. Mater. Res.*, 562-564(2012), p. 167.
- [21] F.M. Yang, L. Wang, S.W. Yin, and Y.H. Li, Effect of the addition of α -Si₃N₄ on the direct nitridation of silicon powder at atmospheric pressure, [in] *Proceedings of the 2012 International Conference on Nanotechnology Technology and Advanced Materials*, Hong Kong, 2012, p. 247.